# Surfactant effects in polytetrafluoroethylene dispersion polymerization

**Bernd Luhmann* and Andrew E. Feiring**

*Central Research and Development Department, Experimental Station, I. E. Du Pont De Nemours & Co. Inc., Wilmington, DE 19880-0328, USA*

*(Received 17 March 1988; revised 12 December 1988; accepted 30 December 1988)*

The polymerization rate, surfactant adsorption behaviour and polymer particle morphology are significantly affected by initial surfactant concentration and polymerization time in the aqueous dispersion polymerization of tetrafluoroethylene. The surfactants are lithium perfluoroalkanoates ($CF_3(CF_2)_nCO_2Li$, $n=5$–8). Both hexagonally shaped and short rod-like particles are formed in early stages of the polymerization when the initial surfactant concentration is below its critical micelle concentration (c.m.c.) An increase in the surfactant chain length and concentration tends to promote formation of hexagons. At longer polymerization times, roughly spherical particles, called cobblestones, form the dominant population. As the initial surfactant concentration is increased past its c.m.c., rod-like particles become the dominant population, with the aspect ratio of the rods increasing as the surfactant concentration increases. As previously reported, the rod-like particles and hexagons are single crystals and dispersions of exclusively rod-like particles can form a separate anisotropic phase.

**(Keywords: polytetrafluoroethylene; dispersion polymerization; perfluorinated surfactants; particle morphology; anisotropic dispersions)**

## INTRODUCTION

Polytetrafluoroethylene (PTFE) fine powder dispersions are obtained by polymerizing tetrafluoroethylene (TFE) in water in the presence of perfluorinated surfactants. Although the surfactant acts primarily as a stabilizing agent to prevent coagulation it can also influence the PTFE particle morphology.

PTFE dispersion particles of differing morphology have been reported[1–14], with three types structurally well established: rod-shaped particles; spherical particles; and, in the case of very low-molecular-weight (*MW*) PTFE, particles resembling small hexagons. All three are characterized by a very high degree of crystallinity. Recently, Chanzy *et al.* described the rod-like particles to be PTFE single crystals with the polymer chains arranged in the direction of the long axis of the rods[12,13]. Spherical dispersion particles are not single-crystalline, but contain numerous crystalline regions. They are assumed to develop from rod-like dispersion particles[13]. Hexagonal-shaped particles constitute a second type of PTFE single crystals, and were obtained solely from dispersion polymerizations yielding very low-molecular-weight PTFE ($DP \sim 30$). The polymer chains are arranged perpendicular to the main surface of the hexagons. The thickness of the hexagon is determined by the length of the polymer chains[14].

The possibility of controlling the PTFE particle size and especially its geometric shape by changing the surfactant type and/or its concentration was first suggested by Berry in the late 1940s[1]. He showed that, besides the approximately spherical PTFE dispersion particles, it is possible to synthesize dispersions of rod-shaped PTFE particles, by polymerizing TFE in the presence of high concentrations (typically some few per cent by weight) of selected fluorinated surfactants. PTFE rods with length-to-diameter ratios as high as 400:1 were reported. Berry showed that the polymer chains are extended in the direction of the long axis of the PTFE rods, a result which was later confirmed by Geil and Rahl *et al.*[5,6]. Rahl *et al.* observed that rod-like PTFE particles are more likely in polymerizations ended at low conversion, while polymerizations performed to high conversion gave mostly spherical particles[6]. PTFE dispersions consisting solely of rod-like particles were obtained by Takehisa *et al.* by radiation-induced polymerization in the presence of high concentrations of perfluorinated surfactants (1 to 10% by weight). In an earlier publication they supposed the shape of the PTFE dispersion particles to be related to the form of the micellar aggregates exhibited by the pure surfactant in water[7]. However, in two later papers they related the PTFE particle morphology to the molecular weight of the PTFE: polymer of low *MW* forms preferably rod-like aggregates, while high-*MW* PTFE emerges in the form of approximately spherical dispersion particles[8,9]. Folda *et al.*[12] describe the formation of PTFE dispersions of only rod-like particles, obtained by polymerizing TFE in the presence of high concentrations of perfluorinated surfactants. PTFE dispersions consisting of rod-like particles of sufficiently high length/diameter ratios were found to undergo phase transformation into anisotropic, liquid-crystalline dispersion phases.

These dispersions[12] contained relatively low-molecular-weight PTFE ($\sim 25\,000$), much less than that of the typical commercial polymer. Although the authors conclude that formation of the rod-shaped particles is

*To whom correspondence should be addressed at: Beiersdorf AG, R&D Division TESA, Unnastrasse 48, D-2000 Hamburg 20, FRG

0032-3861/89/091723-10$03.00

dominated by the action of the surfactant, as did Berry[1] some 40 years earlier, the exact relationship between particle morphology and surfactant concentration remains unclear, particularly with higher-molecular-weight polymer and under carefully controlled conditions. The goal of this work is to get a better understanding of the role which the surfactant plays in the aqueous dispersion polymerization of TFE, and especially to evaluate in more detail the interplay of surfactant kind, its concentration and association into micellar aggregates and the PTFE particle morphology.

## EXPERIMENTAL

### *Perfluoroalkanoic acids*

Perfluoroalkanoic acids $F_3C(CF_2)_{n-2}COOH$ with $n=7, 8, 9$ and 10 were commercially available (Crescent, SCM). Lower homologues with $n=7$ and 8 were purified by fractionation using a 25 cm Vigreux column. Compounds with $n \geq 8$ were purified by sublimation. All acids are white crystalline compounds at room temperature and colourless liquids above their melting points.

### *Lithium perfluoroalkanoates*

Lithium salts of the perfluoroalkanoic acids were prepared by dissolving the acids in water and neutralization with an aqueous LiOH solution to pH 7. In the case of lithium perfluoroheptanoate the aqueous solution was used for all further studies. Lithium salts of the higher homologues were isolated by evaporation of the water using a rotary evaporator. The well dried crude products were recrystallized from a mixture of five parts $CHCl_3$ and two parts of acetone. *Table 1* gives physical data for the lithium perfluoroalkanoates.

### *Tetrafluoroethylene*

Tetrafluoroethylene (TFE) was supplied by Du Pont. The stabilizer (D-limonen) was removed by passing the TFE through silica gel. The absence of D-limonen in the purified TFE was checked by gas chromatography. Stabilizer-free TFE was used within a period of two weeks after removal of the stabilizer.

### *TFE polymerization*

TFE polymerizations were carried out in a 12 oz (~400 ml) glass reaction vessel equipped with a stainless-steel pressure head and a mechanical stainless-steel stirrer (LAB CREST Scientific). An injection/sampling port attached to the pressure head of the reactor allowed injection of initiator under reaction conditions and sampling during the polymerization. Flow sensors in the TFE supply lines were used to measure the TFE gas flow into the reaction vessel. Typical conditions include batch sizes of 200 ml, reaction temperature of +80°C, TFE pressure of 60 psi (414 kPa) and stirring rate of 1000 rpm. Polymerizations were initiated by injection of an aqueous solution containing 10 mg of sodium persulphate. *Figure 1* shows a linear increase of reaction rate with agitation, indicating that the polymerization kinetics are controlled by the transport of the TFE through the gas–liquid interface and/or diffusion within the aqueous phase.

**Table 1** Physical data

| | | M.p. (°C)[a] (microscope) | log (c.m.c.) ($T$=23°C) (mol $l^{-1}$) |
|---|---|---|---|
| Lithium perfluoroheptanoate | (LiC7) | 214 | −1.06 |
| Lithium perfluorooctanoate | (LiC8) | 221 | −1.50 |
| Lithium perfluorononanoate | (LiC9) | 237 | −2.02 |
| Lithium perfluorodecanoate | (LiC10) | 241 | ~−2.42 |

[a] All products melted within a range of 0.5°C

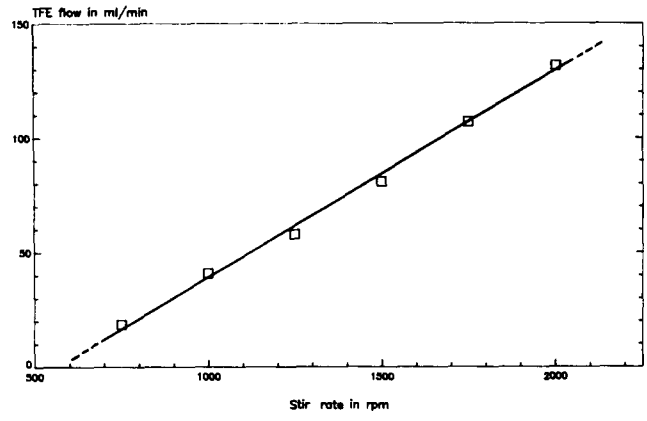


**Figure 1** TFE flow as a function of stir rate. Polymerization batch: 200 ml water, 0.2 g LiC9, 10 mg $Na_2S_2O_8$

### *Description of a typical polymerization*

The desired amount of surfactant and water were weighed into the reaction vessel, and degassed under slow stirring, until the pressure reached the vapour pressure of water. After purging with $N_2$ at 60 psi and with rapid stirring, the degassing procedure was repeated two more times. TFE was allowed to enter the vessel at a pressure of 45 psi, and the vessel was heated to 80°C. After turning the stirrer to the desired speed and after the temperature reached a constant value, the pressure inside the vessel was adjusted to 0.5 psi less than the pressure inside the TFE supply line. The desired amount of initiator, dissolved in 1.5 ml of water, was injected, and the TFE supply line was opened to the vessel, allowing the TFE flow to be recorded. Temperature changes during the reaction, due to the exothermic polymerization process, were countered by changing the depth with which the vessel is immersed in the heating bath. Polymerization was halted by stopping the stirrer and evaporating the TFE from the vessel. PTFE dispersions were broken by freezing. The precipitated polymer was washed thoroughly with water and acetone.

### MW *determination*

Stoichiometric *MW* were calculated from initiator decomposition and polymer yield. For the calculations it was assumed that only thermal decomposition of the persulphate takes place, that every radical formed starts a polymer chain, that chain termination occurs solely by recombination, and that there are no chain transfer processes. Half-life times for persulphate decomposition in aqueous medium were taken from the literature[15].

### *Surface tension measurements*

A Fisher 215 Autotensiomat using the de Nuoy ring method was used for the surface tension measurements. To determine the surface tension of the pure surfactants in water as a function of the surfactant concentration, a

series of samples (15–20) of different surfactant concentration was prepared. The freshly prepared samples (~20 ml batches) were stored prior to use for 14 h in 100 ml covered Pyrex glass beakers. To get reproducible results, the surface tension measurements had to be carried out with low elevator speeds. Surface tensions of the PTFE dispersions were obtained in the same fashion.

*Electron microscopy*

PTFE dispersions were diluted to a total polymer concentration of ~10 g PTFE per litre. To stain the dispersion particles five parts of the diluted dispersions were mixed with one part of an aqueous solution containing 1% phosphotungstic acid (PTA). One drop of the treated dispersions was placed on a microscopic grid and blotted carefully with a cotton tissue, leaving a thin film of negatively stained PTFE.

*D.s.c. measurements*

D.s.c. measurements were carried out using a Du Pont 910 DSC. A heating rate of 10°C $min^{-1}$ and sample sizes of $10 \pm 0.5$ mg were used for all runs.

## RESULTS AND DISCUSSION

*Surfactant effects on rates*

Polymerization of TFE in water, initiated by sodium persulphate, was carried out in the presence of varying concentrations of carefully purified lithium perfluoroheptanoate (LiC7), -octanoate (LiC8), -nonanoate (LiC9) and -decanoate (LiC10) surfactants. *Figure 2* shows typical conversion–time plots for TFE polymerizations carried out in the presence of LiC9. Plotted is the TFE gas flow, as measured at the inlet of the reaction vessel, as a function of the reaction time (injection of the initiator at $t=0$). Surfactant concentrations range from well below to well above the critical micelle concentration (c.m.c.). Two different polymerization regimes can be distinguished depending on whether the reaction is initiated at surfactant concentrations below or above the c.m.c. For runs started below the c.m.c., a short induction period, in the range of 1–2 min is observed before the polymerization begins. After 'kick off' the TFE flow increases slowly to moderate values, and then stays constant at longer reaction times. In contrast, runs started at surfactant concentrations above the c.m.c. exhibit a rapid increase of the TFE uptake almost

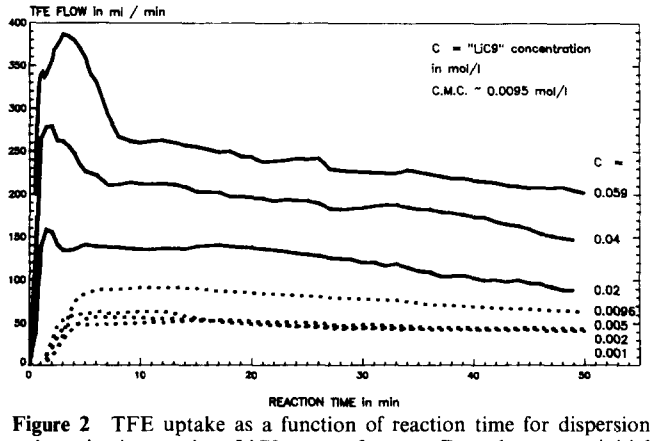


**Figure 2** TFE uptake as a function of reaction time for dispersion polymerizations using LiC9 as surfactant. Dotted curves: initial surfactant concentration below c.m.c. Full curves: initial surfactant concentration above c.m.c.

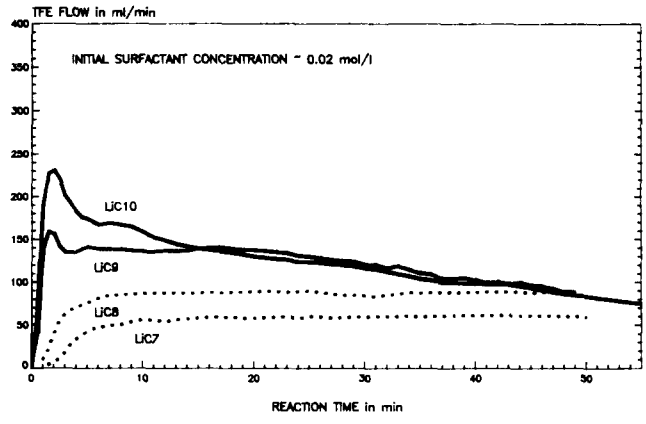


**Figure 3** TFE uptake as a function of reaction time for polymerization runs using initial surfactant concentrations of ~0.02 mol $l^{-1}$ LiC*n*. For dotted and full curves, see legend to *Figure 2*

instantaneously after injection of the initiator solution. The reaction rate passes through a distinct maximum, the maximum being more pronounced at higher surfactant concentrations. At longer reaction times the TFE flow declines slowly. Similar sets of curves were obtained with the other surfactants. For surfactant concentrations well below the c.m.c. the absolute concentration has little influence on the polymerization rate. An increase in reaction rate is first observed as the surfactant concentration approaches the c.m.c., and change in the form of the reaction rate *versus* reaction time curve appears as the surfactant concentration is increased above the c.m.c.

*Figure 3* compares conversion–time plots of polymerizations using different surfactants at the same initial concentrations (0.02 mol $l^{-1}$). This concentration is above the c.m.c. of the nine- and ten-carbon surfactants and below the c.m.c. of the shorter-chain species. Polymerization rates and the form of the conversion–time plots change characteristically according to the rules described above. The overall PTFE yield increases with decreasing c.m.c. of the surfactants, an effect that is a consequence of a general increase in reaction rate as the hydrophobicity of the surfactants increases, plus the presence of high conversions during the early stages of polymerization, when the polymerization is started above the c.m.c.

As indicated in the 'Experimental' section, the polymerization rate is controlled by transport of the TFE to the polymerization site. Changes in reaction rate are attributed mainly to changes in TFE solubility and transport in the aqueous dispersion phase.

Numerical data on polymerizations are summarized in *Table 2*.

*Surface tension measurements*

*Figure 4* shows plots of the surface tension of aqueous solutions of pure surfactants LiC*n* ($n=7$–10) as a function of the log of the surfactant concentration. C.m.c. values were determined by graphical extrapolation of the decreasing and the horizontal branch of the surface tension–log ($c$) functions, and defined as the $x$ value of the intercept. The curve for LiC10 exhibits a distinct minimum at surfactant concentrations around the c.m.c., indicating the presence of impurities. The minimal surface tension was estimated and set equal with the c.m.c.

Knowing the functional relation between surface tension and surfactant concentration for the pure

**Table 2** Dispersion polymerizations: overview of polymerization conditions and product properties

| Run no. | Surfactant type | Surfactant concentration (wt%) | Surfactant concentration (mol $l^{-1}$)[c] | Surfactant concentration (c.m.c. units) | Reaction time (min) | PTFE yield[a] (g) | Stiochiometric *MW* ($10^6$ dalton) | Particle morphology[b] at beginning of reaction C | H | R | Particle morphology[b] at end of reaction C | H | R |
|---|---|---|---|---|---|---|---|---|---|---|---|---|---|
| A-102 | None | – | – | – | 50 | 21.0 | 1.9 | | | | | | |
| B-82 | $LiOOCC_6F_{13}$ | 0.35 | 9.5 (−3) | 0.11 | 50 | 10.4/9.5 | 1.0 | − − | + | o | + | | − |
| B-84 | | 0.70 | 1.9 (−2) | 0.22 | 50 | 11.2/10.4 | 1.1 | | + | − | − | − | + |
| B-86 | | 1.38 | 3.8 (−2) | 0.44 | 50 | 15.3/13.5 | 1.55 | | + | o | | + | + |
| B-98 | | 2.06 | 5.7 (−2) | 0.66 | 50 | 20.9/21.1 | 2.0 | | | + + (s+l) | | + | + |
| B-88 | | 3.38 | 9.6 (−2) | 1.10 | 50 | 30.6/31.4 | 3.1 | | | + + | | | + + (s+l) |
| B-92 | | 4.72 | 1.4 (−1) | 1.59 | 40 | 29.1/29.8 | 3.0 | | | + + | | | + + |
| B-90 | | 6.50 | 2.0 (−1) | 2.27 | 50 | 21.8/21.8 | 2.3 | | | + + | | | + + |
| B-8 | $LiOOCC_7F_{15}$ | 0.087 | 2.1 (−3) | 0.065 | 49 | 11.0/10.0 | 1.3 | | | | | | |
| A-130 | | 0.173 | 4.1 (−3) | 0.13 | 49 | 8.7/8.2 | 0.93 | | + | − | | + | o |
| A-128 | | 0.346 | 8.3 (−3) | 0.26 | 49 | 9.6/9.8 | 1.14 | | + | o | | + | o |
| A-122 | | 0.694 | 1.7 (−2) | 0.52 | 49 | 16.8/16.5 | 1.8 | | + | − | | + | − |
| A-124 | | 1.37 | 3.3 (−2) | 1.05 | 49 | 27.9/25.9 | 2.6 | | | + + (s+l) | | + | + (s+l) |
| A-126 | | 2.71 | 6.5 (−2) | 2.08 | 49 | 50.4/ | 4.3 | | | + + | | | + + |
| A-100 | $LiOOCC_8F_{17}$ | 0.047 | 1.0 (−3) | 0.105 | 50 | 9.9/7.7 | 0.9 | | + | o | − − | + | o |
| A-96 | | 0.094 | 2.0 (−3) | 0.21 | 50 | 9.3/8.2 | 0.86 | | | | − − | + | − |
| A-114 | | 0.094 | 2.0 (−3) | 0.21 | 50 | 8.6/ | | not evaluated | | | | | |
| A-94 | | 0.235 | 5.0 (−3) | 0.52 | 50 | 9.8/9.6 | 0.95 | | + | − | | + | − |
| A-88 | | 0.45 | 9.6 (−3) | 1.00 | 50 | 15.4/15.0 | 1.33 | | + | o | | + | o |
| A-90 | | 0.93 | 2.0 (−2) | 2.1 | 49 | 24.7/24.7 | 2.2 | | | + + (s+l) | | | + (s+l) |
| A-92 | | 1.85 | 4.0 (−2) | 4.1 | 49 | 39.1/39.8 | 2.3 | | | + + | | | + + |
| B-10 | | 2.74 | 5.9 (−2) | 6.2 | 50 | 51.1/47.9 | 4.1 | | | + + | | | + + |
| A-76 | $LiOOCC_9F_{19}$ | 0.026 | 5.0 (−4) | 0.13 | 34 | 5.6/5.2 | 0.82 | | + | o | | + | − |
| A-72 | | 0.052 | 1.0 (−3) | 0.26 | 36 | 5.8/5.1 | 0.83 | | + | − | | + | − |
| A-74 | | 0.104 | 2.0 (−3) | 0.525 | 36 | 7.7/7.1 | 1.02 | | + | − | | + | − − |
| A-66 | | 0.26 | 5.0 (−3) | 1.3 | 48 | 12.8/12.3 | 1.03 | | | + (s+l) | | + | o |
| A-68 | | 0.53 | 1.0 (−2) | 2.7 | 55 | 19.1/17.0 | 1.42 | | | + + | | | + + (s+l) |
| A-78 | | 0.73 | 1.4 (−2) | 3.7 | 55 | 22.2/ | 1.56 | | | + + | | | + + |
| A-70 | | 1.03 | 2.0 (−2) | 5.25 | 55 | 27.8/27.2 | 1.95 | | | + + | | | + + |
| B-28 | | 2.04 | 4.0 (−2) | 10.4 | 49 | 39.4/ | 2.6 | | | + + | | | + + |

[a] First number is PTFE yield as calculated from PTFE uptake; second number gives weight of precipitated polymer
[b] Particle morphology: C = cobblestone-like, H = hexagonal, R = rod-like; − − = very few, − = few, o = some, + = many, + + = exclusively, (s+l) = short + long rods
[c] Number in parentheses is power of 10 by which entry is to be multiplied

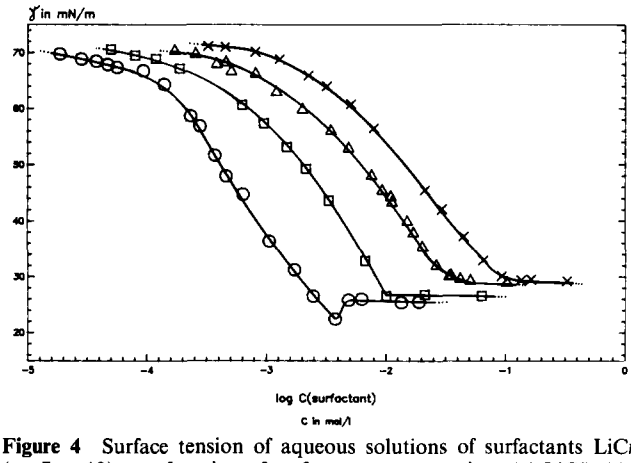


**Figure 4** Surface tension of aqueous solutions of surfactants LiC*n* ($n = 7$ to 10) as a function of surfactant concentration: (x) LiC7; (△) LiC8; (□) LiC9; (○) LiC10

surfactant–water systems allows quantitative measurement of the depletion of surfactants in the aqueous phase during polymerization. It is assumed that the aqueous phase and the PTFE dispersion particles can be treated as separate phases, and that surface tension measurements carried out on dispersions allow selective evaluation of the surfactant concentration in the aqueous phase, i.e. the PTFE itself or surfactant–PTFE aggregates are assumed not to contribute to the surface tension of the dispersions. *Figure 5* shows, for polymerization runs in *Figure 2*, plots of the log of the 'free' (non-adsorbed) surfactant concentration, $c_f$, as a function of polymer yield. In close relation with the results obtained from conversion–time plots it is possible to differentiate between runs started below and those started above the c.m.c. For polymerizations initiated at surfactant concentrations below the c.m.c., log $c_f$ decreases approximately linearly with the polymer yield. The slope of the traces is found to be more negative with lower initial surfactant concentration. For polymerization runs started at surfactant concentrations at or above the c.m.c., log $c_f$ decreases rapidly during the initial stages of polymerization to below the c.m.c., an effect that is more pronounced at lower surfactant c.m.c. Once below the c.m.c., a linear decrease of log $c$ is again observed with increasing polymer yield.

*Figure 6* compares plots of log $c_f$ as a function of polymer yield for polymerizations started at approximately the same initial surfactant concentration, but using different surfactants LiC*n*. Especially conspicuous

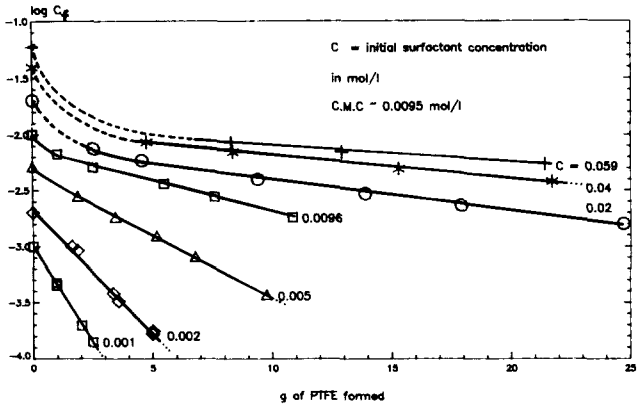


**Figure 5** Free surfactant concentration $c_f$ as a function of polymer yield. Surfactant = LiC9

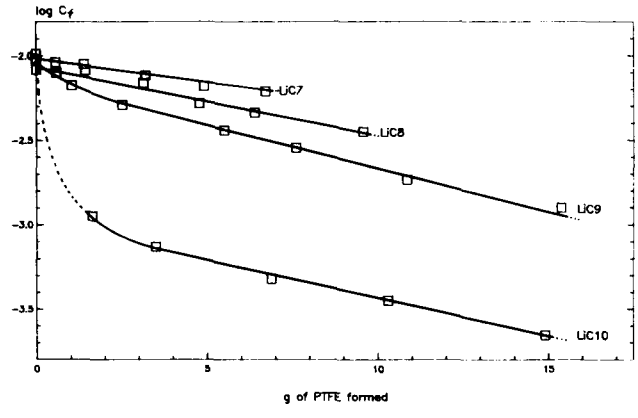


**Figure 6** Free surfactant concentration $c_f$ as a function of polymer yield. Initial surfactant concentration ~0.01 mol $l^{-1}$

is the distinct change in surfactant depletion when going from sub-c.m.c. to super-c.m.c. initial surfactant concentrations.

For interpretation of the surface tension data it was assumed that changes in the value of the c.m.c. between $RT$ (~25°C) and the actual polymerization temperature of +80°C can be neglected. Data obtained by H. Hoffmann *et al.* indicate that the c.m.c. changes only slightly with temperature for these compounds[16].

*Particle morphology*

Electron microscopy was used to follow the PTFE particle morphology. Electron micrographs were taken as a function of surfactant kind, surfactant concentration and reaction time. Essentially three types of PTFE dispersion particles can be distinguished: dispersion particles resembling hexagons; approximately spherical dispersion particles resembling cobblestones; and anisometric, rod-shaped dispersion particles.

PTFE dispersion particles exhibiting sharp edges, which intersect frequently at defined angles of approximately 120°C, resembling small hexagons, are formed during the initial stages of polymerization in runs started below the c.m.c., and form in runs started around or above the c.m.c. during the later stages of polymerization. Particle sizes are typically in the range of 0.04 to 0.2 $\mu$m in diameter at solids contents of the dispersions around ~5% by weight. The small hexagons resemble those reported by Chanzy *et al.*[14]. PTFE chain-folded lamellar single crystals have also been observed for polymer samples cooled very slowly from the melt[17].

Spherical dispersion particles resembling cobblestones are formed in polymerization runs using low concentrations of short-chain surfactants, like LiC7. Particle sizes are in the range of 0.1 to 0.3 $\mu$m at solid contents around 5% by weight. Cobblestone-like dispersion particles were observed exclusively during the later stages of polymerization, indicating that they evolve from hexagonal and/or short rod-like dispersion particles.

Rod-like dispersion particles develop at all surfactant concentrations from well below to well above the c.m.c. In the case of polymerizations initiated at surfactant concentrations below the c.m.c., rods seem to form less frequently with increasing surfactant content and increasing surfactant chain length. However, rod-like particles establish the sole population in the case of polymerizations initiated well above the c.m.c. Rods formed below the c.m.c. display a broad width distribution. Widths lie in the range of 10 to 100 nm at solids contents around 5% by weight. Length-to-diameter ratios are in general in the range of 3:1 to 10:1. The average particle size does not change much with surfactant content and surfactant chain length. Individual particles formed in the sub-c.m.c. regime often look distorted: their width may change abruptly, backfolding may occur, rods may end up in spherical structures, or may simply be rolled up, resembling in the latter case isometric dispersion particles. Rod-like PTFE particles which emerge in polymerizations started above the c.m.c. are on the other hand generally very homogeneous in width. Particle widths are typically in the range of 10 to 100 nm at solids contents between 10 and 20% by weight. During the initial stages of polymerization rods having widths as low as ~5 nm have been detected. Average particle widths of the rods decrease distinctly with increasing initial surfactant concentration, indicating the formation of more and/or longer PTFE particles with rising surfactant content. Length-to-diameter ratios of the rods may vary between little above unity to at least 100:1, and increase with increasing surfactant concentration. Phase separation into an optically isotropic and an optically anisotropic, liquid-crystalline (LC) dispersion phase may occur (see below) with rods of higher $l/d$ ratios assembled preferably in the LC phase. Runs started slightly above the c.m.c. often show the presence of a bimodal length distribution of the rods, showing numerous short rod-like particles of $l/d$ ratios around 2:1 to 4:1 and fewer long rod-like particles of $l/d$ ratios >10:1.

Four different sets of electron micrographs are presented. The first two sets (*Figures 7* and *8*) monitor the PTFE particle morphology as a function of surfactant concentration. Surfactants are LiC7 and LiC9. Reaction times are 49–50 min unless otherwise indicated. Set three (*Figure 9*) shows electron micrographs of PTFE particles formed during the very early stages of polymerization at surfactant concentrations slightly below, at and slightly above the c.m.c. Reactions were carried out in the presence of LiC9. Set four (*Figure 10*) presents electron micrographs showing the time evolution of particle morphology, for a polymerization reaction started little above the c.m.c., using LiC10 as surfactant.

*LiC7 surfactant. Figures 7a–e* present electron micrographs of PTFE particles formed in polymerization runs using LiC7 as surfactant (runs B-82 to B-98). At very low surfactant concentrations (*Figure 7a*) relatively large dispersion particles of diverse shape are formed. Ball-like

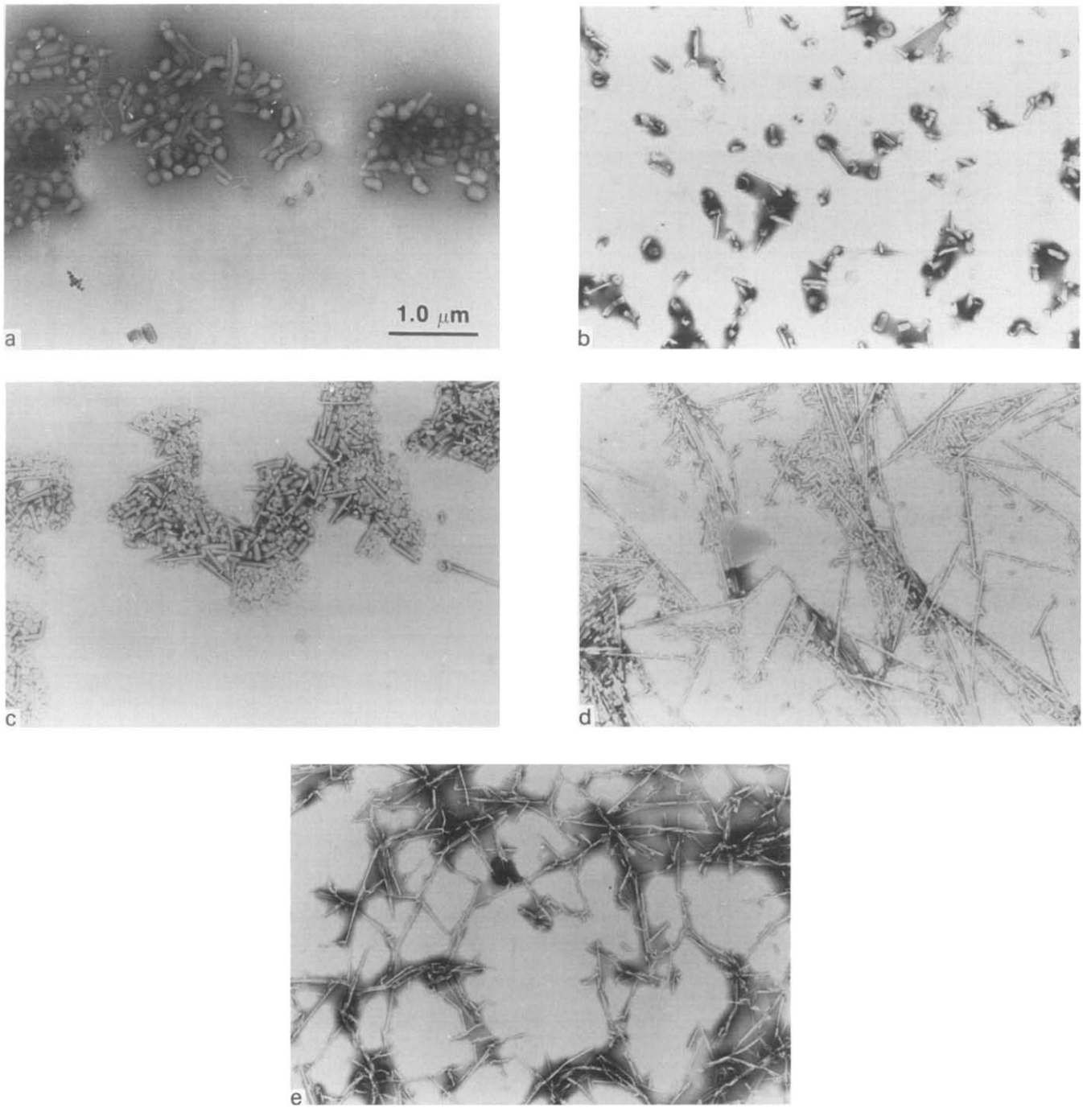


**Figure 7** Electron micrographs of PTFE dispersion particles. Surfactant = LiC7. Polymerizations: (a) B-82; (b) B-84; (c) B-86; (d) B-88; (e) B-92

or ellipsoidal particles resembling typical cobblestones can be distinguished from more rod-like entities. Cobblestone-like dispersion particles show diameters up to 0.3 μm. With increasing surfactant concentration (*Figures 7b* and *7c*) cobblestone-like particles vanish. The average particle diameter of the particles decreases slightly. Essentially two types of particles can be discerned: dispersion particles resembling small hexagons in structure; and rod-shaped particles of relatively low *l/d* ratios. Rod-shaped particles appear more frequently at low surfactant concentrations (*Figure 7b*), while hexagonal structures emerge more frequently at higher surfactant concentrations (*Figure 7c*). When approaching the c.m.c. relatively long rod-shaped dispersion particles are present for the first time, and at surfactant concentrations around the c.m.c. a distinct change in PTFE particle morphology occurs. Polymerizations initiated in the super-c.m.c. range (*Figures 7d* and *7e*) yield exclusively rod-like dispersion particles. Particle diameters decrease significantly with increasing initial surfactant content. Pictures from samples polymerized at surfactant concentrations slightly above the c.m.c. imply a bimodal length distribution of the rods. Dispersions undergoing phase separation into an optically anisotropic liquid-crystalline (LC) dispersion phase and an optically isotropic common dispersion phase display a marked accumulation of rod-like particles of high *l/d* ratios within the LC phase.

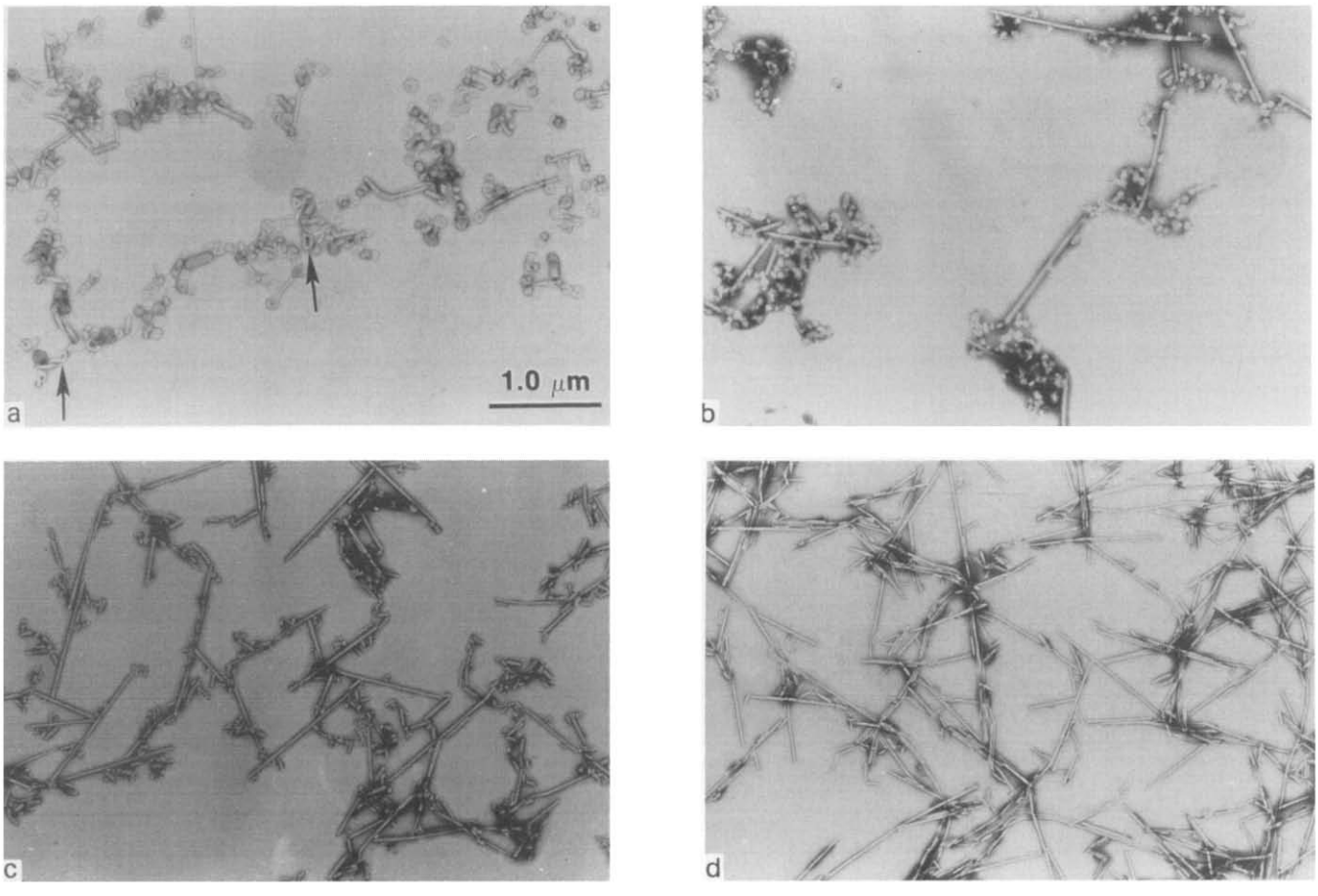


**Figure 8** Electron micrographs of PTFE dispersion particles. Surfactant = LiC9. Polymerizations: (a) A-100; (b) A-88; (c) A-114; (d) B-10. Arrows indicate backfolded rods

*LiC9 surfactant*. With increasing surfactant chain length cobblestone-like dispersion particles are formed less frequently. The main particle population in runs using sub-c.m.c. concentrations of LiC9 (runs A-88 to A-114 and B-10) are hexagonal dispersion particles. Rod-shaped particles appear less often. Some of the rods in *Figure 8a* show backfolding (indicated by arrows). In accordance with the results obtained from runs using LiC7 as surfactant, a drastic change in particle morphology occurs at surfactant concentrations around the c.m.c.: runs started at the c.m.c. show the appearance of rod-shaped particles of comparably high $l/d$ ratios (*Figure 8b*); rods form the sole population in the case of polymerizations started at initial surfactant concentrations above the c.m.c. (*Figures 8c* and *8d*). A bimodal size distribution seems to be present for samples polymerized at surfactant concentrations slightly above the c.m.c.

*LiC9 surfactant and short reaction times*. To examine the change in particle morphology that occurs at surfactant concentrations around the c.m.c. in more detail, polymerizations were initiated at initial surfactant concentrations (surfactant = LiC9) of $0.7 \times$ c.m.c., $1 \times$ c.m.c. and $1.4 \times$ c.m.c. *Figures 9a–c* present electron micrographs of dispersion samples taken very early after initiation of the polymerizations. Below the c.m.c. numerous isometric dispersion particles, which are assumed to be the precursor of the hexagonal particles, as well as several long rod-shaped particles, can be detected. Exclusively rod-like particles are formed at the c.m.c. However, a clear distinction between short rods and those of high $l/d$ ratios is possible. Short rods appear in place of the isometric dispersion particles. Short rods are often slightly fatter than long rods. Towards higher surfactant concentrations a general increase of the average $l/d$ ratio of the rods is seen. The particle thickness seems to be somewhat lower compared with the two other runs.

*PTFE particle morphology as a function of reaction time*

*Figures 10a* and *10b* follow the PTFE particle morphology for a polymerization run (A-66) initiated at an initial Li perfluorodecanoate concentration of $\sim 1.3 \times$ c.m.c. During the initial stages of polymerization (*Figure 10a*) the particle population consists entirely of rod-like dispersion particles with numerous short rods and fewer long rods. With increasing reaction time (*Figure 10b*) the short rods disappear, being substituted by hexagonal dispersion particles, while long rods are present throughout the reaction. The described behaviour indicates that the hexagonal particles evolve in the present case out of the short rod-like particles, by growth of the latter in the direction of their short axis.

*Formation of anisotropic, liquid-crystalline PTFE dispersions*

PTFE dispersions obtained from polymerization runs using initial surfactant concentrations well below the c.m.c. display very little flow birefringence, indicating the presence of only slight amounts of anisometric,

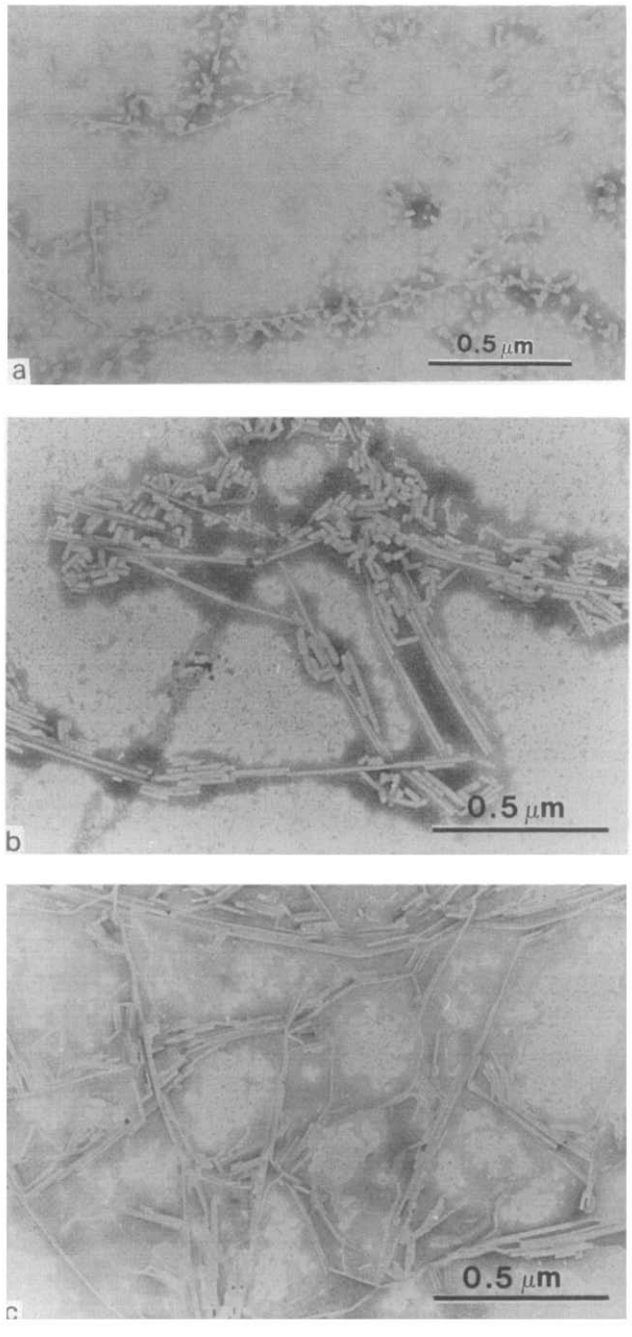


**Figure 9** Electron micrographs of PTFE dispersion particles. Samples taken very early during polymerization. Surfactant = LiC9. (a) Reaction time = 120 s, initial LiC9 concentration = 0.7 × c.m.c.. (b) Reaction time = 90 s, initial LiC9 concentration = 1.0 × c.m.c. (c) Reaction time = 60 s, initial LiC9 concentration = 1.3 × c.m.c.

rod-shaped PTFE particles of high $l/d$ ratios. With increasing initial surfactant content a strong increase in flow birefringence is observed when approaching the c.m.c. Using initial surfactant concentrations above the c.m.c., it is possible to obtain PTFE dispersions that undergo phase separation into an optically isotropic, but strongly flow-birefringent dispersion phase, and an optically anisotropic, liquid-crystalline (LC) dispersion phase. The LC phase is of higher density than the optically isotropic phase and therefore separates as the lower phase. Optical microscopic textures of the birefringent phase are very similar throughout. Sheared samples tend to align in a homogeneous orientation. LC phases display as characteristic behaviour a marked viscoelasticity. On diluting the LC phases with water, these can be transformed into common, non-LC but strongly flow-birefringent dispersions.

*Table 3* presents an overview on phase-separated PTFE dispersions. The amount of LC phase obtained in a given run increases with increasing surfactant content. Surfactants with a longer hydrophobic unit, at the same initial surfactant concentration, are more efficient in providing high amounts of LC dispersion phases.

*Thermal behaviour*

*Figure 11* presents d.s.c. traces of virgin PTFE samples monitored in a temperature range between −10 and +40°C. The traces are arranged as a function of type and concentration of the surfactant which has been present during the polymerization process.

Virgin PTFE samples obtained by polymerizing TFE in an aqueous medium, either in the absence of surfactant (polymer sample from precipitated PTFE), or at surfactant concentrations above the c.m.c., show the presence of an exothermic phase transformation I around +20°C (maximum) and a weaker transformation II around +30°C (maximum), the latter appearing as a shoulder on the main peak. Passing the c.m.c. towards lower surfactant contents a third exothermic peak I′ splits off from transformation I towards its lower-temperature side. The relative intensities of transformations I and I′ change in a characteristic manner with surfactant chain length and surfactant concentration. While peak I dominates for samples polymerized in the presence of LiC7, peak I′ gains significance with increasing surfactant

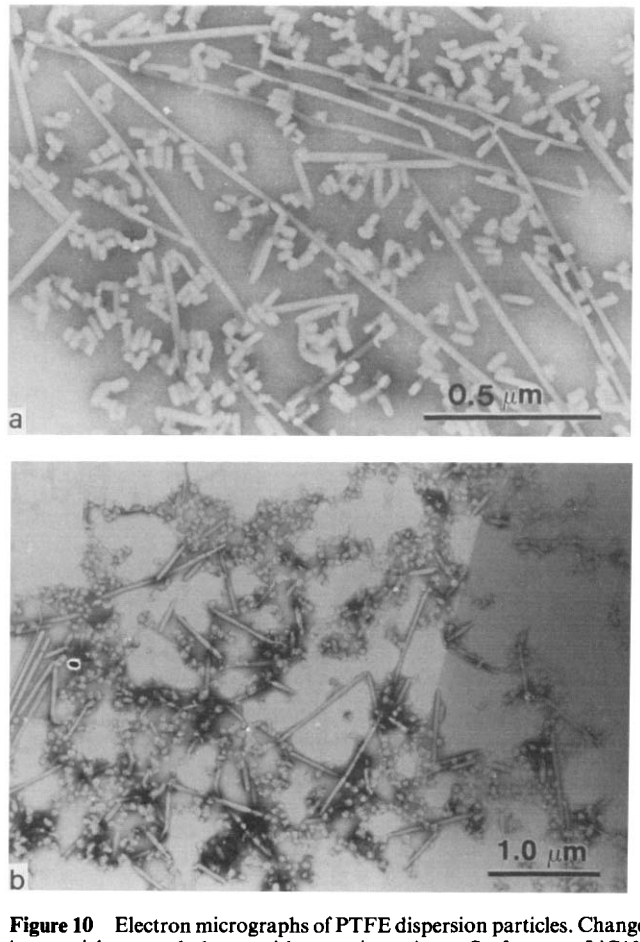


**Figure 10** Electron micrographs of PTFE dispersion particles. Change in particle morphology with reaction time. Surfactant = LiC10. Polymerization A-66. Reaction times: (a) 5 min; (b) 48 min

**Table 3** Survey of phase-separated PTFE dispersions: for reaction times and yields see *Table 2*

| Run no. | Surfactant | Phase separation | LC phase (vol%) | Initial surfactant content | |
|---|---|---|---|---|---|
| | | | | (mol l$^{-1}$) | (c.m.c. units) |
| B98 | Li perfluoroheptanoate | – | 0 | 0.057 | 0.66 |
| B-88 | | + | 4.5 | 0.096 | 1.1 |
| B-92 | | + | 27.6 | 0.14 | 1.59 |
| B-90 | | + | 14.6 | 0.2 | 2.27 |
| A-122 | Li perfluorooctanoate | – | 0 | 0.017 | 0.52 |
| A-124 | | + | <1 | 0.033 | 1.05 |
| A-126 | | + | 16.6 | 0.065 | 2.1 |
| A-88 | Li perfluorononanoate | – | 0 | 0.0096 | 1 |
| A-90 | | + | 4 | 0.02 | 2.1 |
| A-92 | | + | 15.4 | 0.04 | 4.1 |
| B-10 | | + | 36.9 | 0.059 | 6.2 |
| A-66 | Li perfluorodecanoate | – | 0 | 0.005 | 1.3 |
| A-68 | | + | <1 | 0.01 | 2.7 |
| A-78 | | + | ~1 | 0.014 | 3.7 |
| A-70 | | + | not evaluated | 0.02 | 5.2 |
| B-28 | | + | 15.5 | 0.04 | 10.4 |

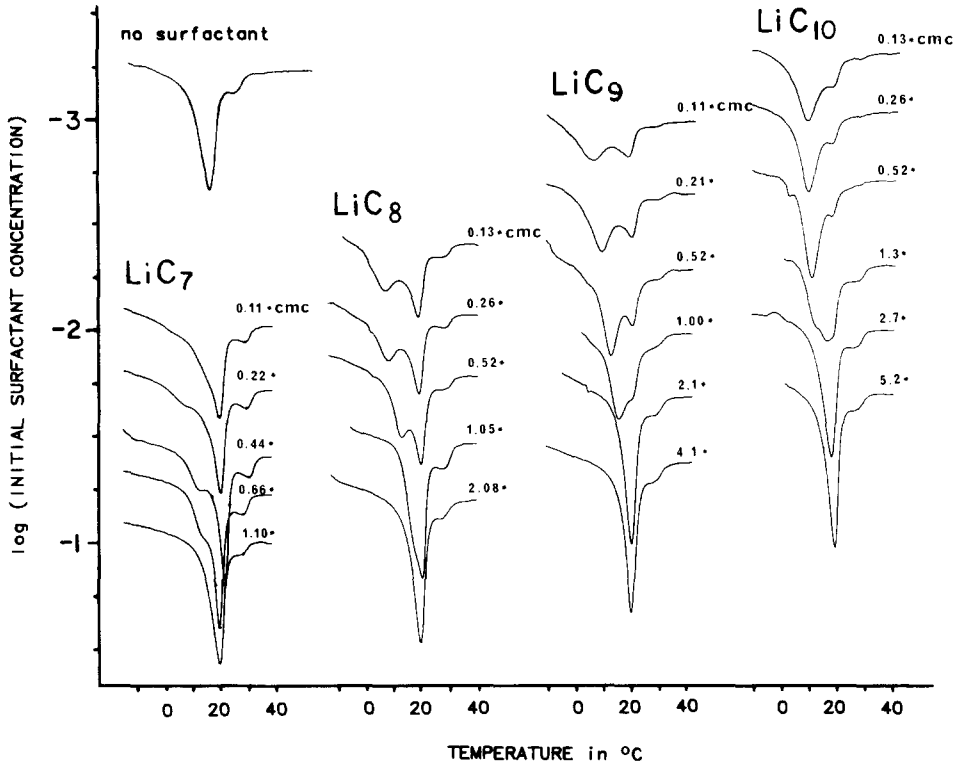


**Figure 11** D.s.c. traces of virgin PTFE. Traces arranged as function of type and concentration of the surfactant, which has been present during the polymerization process. Baseline at 40°C adjusted to the concentration axis

chain length, and becomes the major transformation peak in the case of PTFE samples polymerized in the presence of LiC10.

D.s.c. traces of PTFE samples heated above their melting point display only a single peak around +23°C with the shoulder towards the high-temperature side. Since differences of the d.s.c. traces appear only for virgin PTFE samples, and since a major change of the form of the traces appears around the c.m.c., it is supposed that the changes relate to particles of different morphology. Rod-like and cobblestone dispersion particles are assigned to transformation peak I. The appearance of transformation peak I′ is attributed to the hexagonal dispersion particles, and in qualitative agreement with the electron micrographic observations transformation I′ gains weight in the sub-c.m.c. regime with increasing surfactant chain length and increasing surfactant concentration. In accordance with these assumptions

PTFE dispersions obtained by polymerizing TFE in the absence of surfactant consist essentially of rod-like dispersion particles of low $l/d$ ratios. Polymer samples consisting preferably of cobblestone-like dispersion particles exhibit solely transformation peak I. However, a distinct broadening of the peak is observed towards its low-temperature side, which may refer to the observation that the latter type of particle is formed only during the later stages of polymerization, evolving from hexagonal and short rod-like dispersion particles.

## CONCLUSIONS

The results of this work reveal a distinct correlation between the state of aggregation of the surfactant during the initial stages of polymerization and the PTFE particle morphology. The presence of two different polymerization regimes, which are correlated with the absence or presence of micelles during the early stages of polymerization, are confirmed by the observation of distinct qualitative differences in particle morphology, reaction rate, depletion of free surfactant with polymer yield, and the thermal behaviour of the precipitated virgin PTFE as monitored by d.s.c.

The phenomenon that dispersion particle size and shape change distinctly at concentrations near the critical micelle concentration of the surfactants suggests that particle nucleation is different in the two regimes. In accordance with standard emulsion polymerization it is assumed that at sub-c.m.c. surfactant concentrations final PTFE dispersion particles evolve from a homogeneous nucleation step, while in the presence of micelles growing PTFE molecules attain micelle kinetics with final PTFE dispersion particles evolving from a heterogeneous nucleation step.

At low reaction times, hexagonal PTFE dispersion particles are only formed in reactions started in the range of sub-c.m.c. surfactant concentrations. Higher surfactant concentration and an extension of the hydrophobic part of the amphiphile favour the formation of hexagons over small rod-like dispersion particles. Both parameters relate to an increase in interaction between surfactant molecules and the growing fluoropolymer chain, stressing the importance of the surfactant in the formation of this type of particle. The observation of Chanzy *et al.* that very low-molar-mass PTFE ($DP \sim 30$) yields PTFE-dispersion particles with a related shape and molecular arrangement of polymer molecules may suggest that low-molar-mass PTFE, which is formed during the initiation process of the polymerization, may act as a template for proper hexagons[14].

With initial surfactant concentrations above the c.m.c., exclusively rod-shaped dispersion particles are present during the early stages of polymerization, with $l/d$ ratios of the rods increasing with increasing initial surfactant concentration. Experiments monitoring the shape of the PTFE dispersion particles with time — in runs using initial surfactant concentrations at or little above the c.m.c. — show that hexagonal dispersion particles arise in this case from short rod-like entities by lateral growth of the latter, indicating a continuous transition between both types of particles. Taking into account that TFE polymerizations carried out in F-113 (1,1,2-trichlorotrifluoroethane) using a fluorocarbon-soluble initiator system yield mostly rod-shaped PTFE particles, the micelles act primarily as a protection of the growing PTFE chains against the aqueous environment and/or as a TFE reservoir (by means of solubilizing the TFE), providing a high local concentration of TFE[18].

Cobblestone-like dispersion particles emerge only during the later stages of polymerization in runs using low concentrations of short-chain surfactant, i.e. under conditions where only little stabilization of the dispersion particles by the surfactant is possible. In accordance with the results obtained by Chanzy *et al.* cobblestone-like dispersion particles are thought to be formed by inter- and intraparticular agglomeration of rod-like and/or hexagonal PTFE dispersion particles.

The present work does not take into account any changes in particle morphology due to alterations in initiator concentration. Preliminary results from polymerization runs carried out at slightly lower temperatures, and lower Na persulphate concentration, indicate that changes in particle morphology can also be induced by changing the initiator concentration: again a general change in particle size from small particles to rod-like dispersion particles of very high $l/d$ ratios is observed at the c.m.c. However, nearly exclusively rod-like dispersion particles of low $l/d$ ratios emerge in the sub-c.m.c. regime. Hexagonal dispersion particles are rare. It is assumed that changes in particle morphology are correlated with an increase in polymerization rate per growing polymer chain. The latter is easily varied in the present case since polymerization kinetics is diffusion-controlled. Polymerization kinetics may present the general feature determining the particle morphology in PTFE dispersion polymerization.

## ACKNOWLEDGEMENTS

We thank M. J. and M. L. vanKavelaar for their electron microscopy work and H. W. Starkweather for many helpful discussions.

## REFERENCES

1 Berry, K. L. US Patent 2559750, July 1951
2 Bunn, C. W., Cobbold, A. J. and Palmer, R. P. *J. Polym. Sci.* 1958, **28**, 365
3 Grimaud, E., Sanlaville, J. and Troussier, N. *J. Polym. Sci.* 1958, **31**, 525
4 Sperati, C. A. and Starkweather, H. W. *Adv. Polym. Sci.* 1961, **2**, 465
5 Geil, P. H. in 'Polymer Single Crystals', Polymer Reviews 5 (Eds. H. F. Mark and E. H. Immergut), Wiley Interscience, New York, 1963
6 Rahl, F. J., Evanco, M. A., Fredericks, R. J. and Reimschuessel, A. C. *J. Polym. Sci.* (*A*-2) 1972, **10**, 1337
7 Takehisa, M., Suwa, T., Seguchi, T. and Tamura, N. *Kokai* 49-27587, Patent Application July 1972, Application No. 47-67565
8 Suwa, T., Takehisa, M. and Machi, S. *J. Polym. Sci.* 1974, **18**, 2249
9 Seguchi, T., Suwa, T., Tamura, N. and Takehisa, M. *J. Polym. Sci., Polym. Phys. Edn.* 1974, **12**, 2567
10 Yamaguchi, S. and Shimizu, T. *Kobunshi Ronbunshu* 1982, **39**(5), 339
11 Yamaguchi, S. *Kobunshi Ronbunshu* 1984, **41**(7), 407
12 Folda, T., Hoffmann, H., Chanzy, H. and Smith, P. *Nature* 1988, **333**, 55
13 Chanzy, H. D. and Smith, P. *J. Polym. Sci., Polym. Lett. Edn.* 1986, **24**, 557
14 Chanzy, H., Folda, T., Smith, P. and Gardner, K. *J. Mater. Sci. Lett.* 1986, **5**, 1045
15 'Polymer Handbook' (Eds. J. Brandrup and E. H. Immergut), Wiley, New York, 2nd Edn., 1975
16 Hoffmann, H. and Ulbricht, W. *Z. Phys. Chem.* (*NF*) 1977, **106**, 167
17 Symons, N. K. J. *J. Polym. Sci.* (*A*) 1963, **1**, 2843
18 Wheland, R., E. I. Du Pont de Nemours, Experimental Station, unpublished results